Myopic (HD-PTP, PTPN23) selectively regulates synaptic neuropeptide release

Dinara Bulgari[a], Anupma Jha[a], David L. Deitcher[b], and Edwin S. Levitan[a,1]

[a]Department of Pharmacology and Chemical Biology, University of Pittsburgh, Pittsburgh, PA 15261; and [b]Department of Neurobiology and Behavior, Cornell University, Ithaca, NY 14853

Edited by Charles F. Stevens, The Salk Institute for Biological Studies, La Jolla, CA, and approved January 2, 2018 (received for review September 25, 2017)

Neurotransmission is mediated by synaptic exocytosis of neuropeptide-containing dense-core vesicles (DCVs) and small-molecule transmitter-containing small synaptic vesicles (SSVs). Exocytosis of both vesicle types depends on Ca^{2+} and shared secretory proteins. Here, we show that increasing or decreasing expression of Myopic (mop, HD-PTP, PTPN23), a Bro1 domain-containing pseudophosphatase implicated in neuronal development and neuropeptide gene expression, increases synaptic neuropeptide stores at the *Drosophila* neuromuscular junction (NMJ). This occurs without altering DCV content or transport, but synaptic DCV number and age are increased. The effect on synaptic neuropeptide stores is accounted for by inhibition of activity-induced Ca^{2+}-dependent neuropeptide release. cAMP-evoked Ca^{2+}-independent synaptic neuropeptide release also requires optimal Myopic expression, showing that Myopic affects the DCV secretory machinery shared by cAMP and Ca^{2+} pathways. Presynaptic Myopic is abundant at early endosomes, but interaction with the endosomal sorting complex required for transport III (ESCRT III) protein (CHMP4/Shrub) that mediates Myopic's effect on neuron pruning is not required for control of neuropeptide release. Remarkably, in contrast to the effect on DCVs, Myopic does not affect release from SSVs. Therefore, Myopic selectively regulates synaptic DCV exocytosis that mediates peptidergic transmission at the NMJ.

secretory granule | peptidergic neurotransmission | motoneuron

Neurons release neuropeptides via the regulated exocytosis of dense-core vesicles (DCVs) to evoke or modulate behavior. Release of neuropeptides with small-molecule transmitters packaged in small synaptic vesicles (SSVs) in the same terminal produces cotransmission that enhances behavioral flexibility (1). Activity-dependent exocytosis of DCVs and SSVs shares many features, including requirements for Ca^{2+} and several secretory proteins, including SNAREs (soluble *N*-ethylmaleimide–sensitive factor attachment protein receptors), Munc-18, synaptotagmin, and CATCHR (complex associated with tethering containing helical rods) domain priming proteins (2–5). Individual neuron subtypes vary in expression of isoforms of the above proteins, but there is no evidence for a different exocytosis protein mediating release from SSVs and DCVs in an individual neuron. Indeed, although knockouts can produce quantitatively different effects on release mediated by SSVs and DCVs, no gene has been identified that qualitatively distinguishes synaptic exocytosis by SSVs and DCVs in mammalian synapses.

To identify genes that regulate synaptic neuropeptide storage and release, we screened for effects of knockdown of phosphatase-related proteins on GFP-tagged neuropeptide fluorescence at the *Drosophila* neuromuscular junction (NMJ). Here, we identify Myopic (mop), the *Drosophila* ortholog of HD-PTP/PTPN23, as a regulator of synaptic neuropeptide storage. Previously, Myopic has been identified as a catalytically inactive pseudophosphatase that shuttles between the nucleus and cytoplasm and also is present near early endosomes, where it recruits the oncoprotein Yorkie and participates in endosomal sorting complex required for transport (ESCRT) function (6–11). ESCRT has been implicated in Myopic regulation of receptor signaling and neuron pruning (e.g., refs. 6, 7, 12, 13), while nuclear function is likely involved in Myopic control of survival motor neuron complex localization (11) and neuropeptide gene transcription (14). Here, we expand the impact of Myopic to synaptic neuropeptide accumulation and show that this effect is not due to a change in neuropeptide synthesis, packaging, or delivery. Rather, Myopic participates in synaptic release from DCVs, but not SSVs.

Results

Myopic Controls Synaptic Neuropeptide Accumulation. We examined presynaptic levels of GFP-tagged *Drosophila* insulin-like peptide 2 (Dilp2-GFP) (15) driven by the native neuronal synaptobrevin promoter in type Ib boutons at the muscle 6/7 NMJ in filleted third-instar larvae. Dilp2-GFP is used here as a DCV marker, as Dilp2 is not normally expressed in motor neurons. RNAi knockdown of Myopic with the motoneuron driver OK6-GAL4 produced an 89 ± 5% increase in synaptic GFP-neuropeptide fluorescence (n = 38 boutons from five animals; Fig. 1 *A* and *B*). Then, we examined the effect of Myopic upregulation, again using the native synaptobrevin promoter to drive Dilp2-GFP expression and OK6 to drive Myopic overexpression. While knockdown and overexpression typically produce opposing results, overexpression of Myopic produced a similar effect as knockdown: The synaptic neuropeptide signal increased by 69 ± 4% (n = 48 boutons from five animals; Fig. 1 *C* and *D*). An increase was also obtained with OK6-GAL4–induced expression of the GFP-tagged neuropeptide. Therefore, these experiments suggest that Myopic regulates synaptic neuropeptide storage.

Significance

Neurotransmission relies on exocytosis of two vesicle types: small synaptic vesicles (SSVs) that contain small-molecule transmitters and dense-core vesicles (DCVs) that contain neuropeptides. The secretory apparatus for synaptic exocytosis has appeared to be conserved for the two vesicle types. This study at the fruit fly neuromuscular junction shows that up- or down-regulating the multifunctional protein Myopic increases synaptic neuropeptide stores by selectively reducing synaptic neuropeptide release evoked by electrical activity or cAMP. In contrast, SSV-mediated release is not affected by Myopic. These results show that Myopic, which is already implicated in neuropeptide gene expression, selectively participates in exocytosis of synaptic DCVs.

Author contributions: D.B., D.L.D., and E.S.L. designed research; D.B., A.J., and D.L.D. performed research; D.B., A.J., D.L.D., and E.S.L. analyzed data; and E.S.L. wrote the paper.

The authors declare no conflict of interest.

This article is a PNAS Direct Submission.

Published under the PNAS license.

[1]To whom correspondence should be addressed. Email: elevitan@pitt.edu.

This article contains supporting information online at www.pnas.org/lookup/suppl/doi:10.1073/pnas.1716801115/-/DCSupplemental.

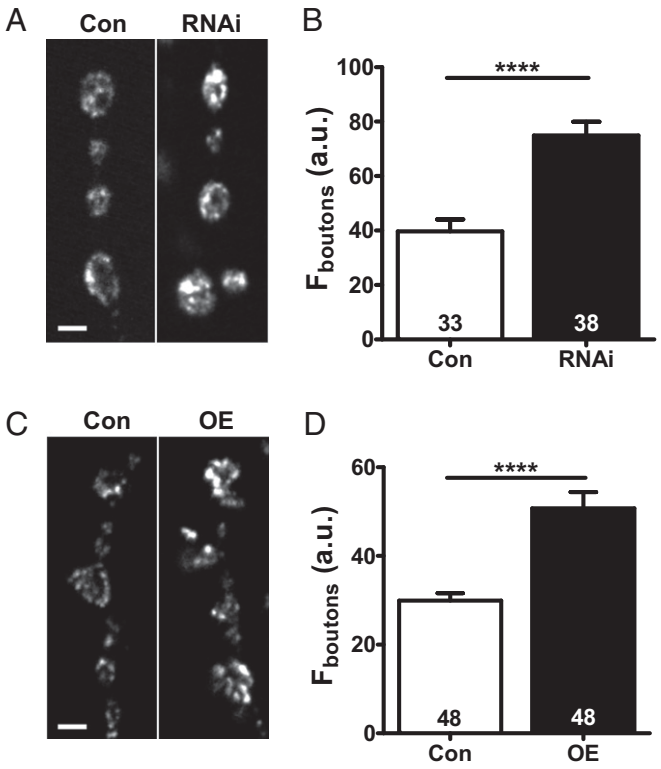

Fig. 1. Myopic controls synaptic neuropeptide accumulation. (*A*) Contrast-enhanced images of Dilp2-GFP–labeled type Ib boutons in control (Con) and Myopic RNAi knockdown (RNAi, no. 34085) NMJs. (Scale bar, 2 μm.) (*B*) Quantification of bouton fluorescence (F). Numbers on the bars indicate the number of boutons analyzed from five animals. (*C*) Representative images of type Ib boutons in Con and Myopic-overexpressing (OE) NMJs with Dilp2-GFP. (Scale bar, 2 μm.) (*D*) Quantification of bouton F. Numbers on the bars represent the number of boutons examined from six animals. ****$P < 0.0001$, unpaired *t* test.

We then considered the mechanism underlying the increase in synaptic neuropeptide accumulation. Imaging DCVs undergoing transport between synaptic boutons (15, 16) showed that DCV content, measured as the fluorescence of transport puncta, was unaffected by Myopic knockdown or overexpression (Fig. S1*A*). Likewise, anterograde and retrograde DCV fluxes were unaffected by altering Myopic expression (Fig. S1*B*). In principle, greater neuropeptide storage per bouton could reflect a change in bouton size. However, there was also no change in bouton area upon Myopic up- or down-regulation (Fig. S1*C*). Together, these results imply that the increase in synaptic neuropeptide in Myopic-overexpressing and -deficient motoneurons is not accounted for by altered DCV content, transport, or bouton size, but is consistent with an increase in synaptic DCV number.

Myopic Inhibits Activity-Induced Synaptic Neuropeptide Release. If the increase in neuropeptide storage stems from decreased secretion, then one would expect an accumulation of older DCVs in boutons. To explore this possibility, we examined a neuropeptide-timer construct [atrial natriuretic factor tagged with monomeric Kusabira Green Orange (ANF-mK-GO) driven by 386Y-GAL4] that converts from green to red fluorescence over hours (17–19). Green/red fluorescence ratios showed that Myopic knockdown or overexpression each produces older DCVs compared with control animals (Fig. 2).

Because inhibition of release could produce this effect, we tested the hypothesis that DCV-mediated neuropeptide release depends on optimal Myopic expression. Specifically, release was measured as the loss of Dilp2-GFP induced by 70-Hz motor nerve electrical stimulation for 1 min. These experiments showed that the two RNAi knockdown constructs tested each markedly inhibited activity-induced neuropeptide release (Fig. 3 *A*–*C*). We then sought to test whether a Myopic mutant could produce a similar effect. However, strong Myopic mutants such as T482 (12) are lethal when combined with a Myopic deficiency, but are viable and do not affect release as a heterozygote (Fig. 3*E*, T482/+). Therefore, we examined the effect of a heteroallelic combination with a weaker Myopic mutation. For this purpose, we used a p-element insertion (P{EPgy2}mop^{EY06090}), which is viable as a homozygote or in combination with a Myopic deficiency and had no effect on release as a heterozygote. However, heterozygotes of two mutants (T482/P) inhibited release (Fig. 3 *D* and *E*), thus verifying Myopic regulation of neuropeptide release. Finally, Myopic overexpression also inhibited activity-induced neuropeptide release (Fig. 3 *F* and *G*). Therefore, multiple genetic perturbations suggest that the greater neuropeptide

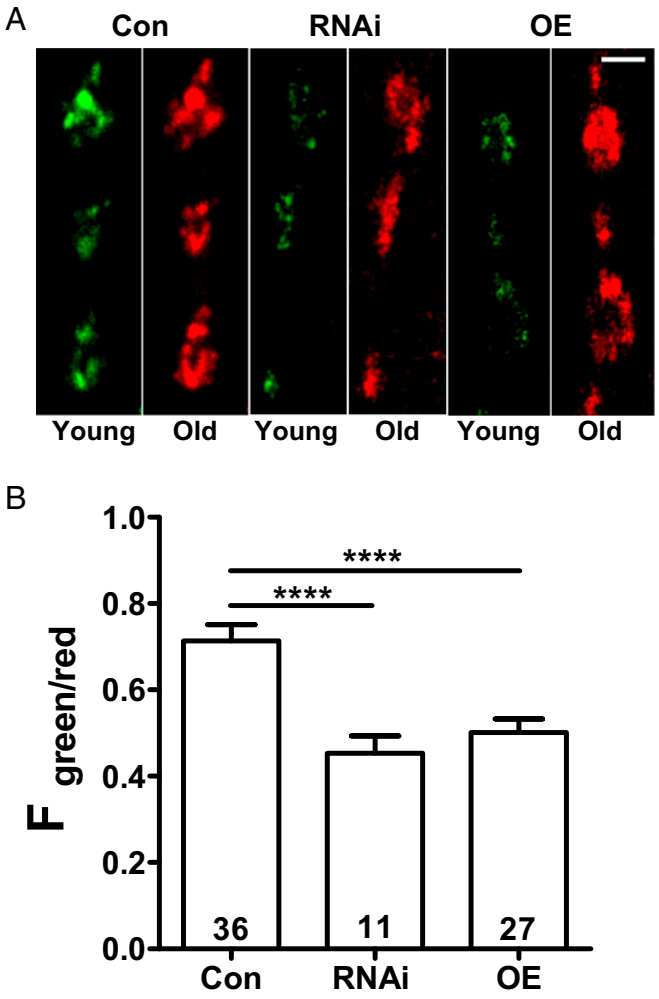

Fig. 2. Age-dependent labeling of DCVs expressing ANF tagged with mK-GO in synaptic boutons. (*A*) Green (young) and red (old) images are shown side by side for control (Con) boutons, Myopic RNAi knockdown (RNAi), and overexpressing (OE) boutons. The contrast was adjusted to normalize red images. (Scale bar, 2 μm.) (*B*) Quantification of green-to-red fluorescence (F) ratio in Con (four animals), RNAi (no. 34085, three animals), and OE (four animals) NMJs. Numbers on the bars represent the number of boutons analyzed. ****$P < 0.0001$, ANOVA with Dunnett's posttest.

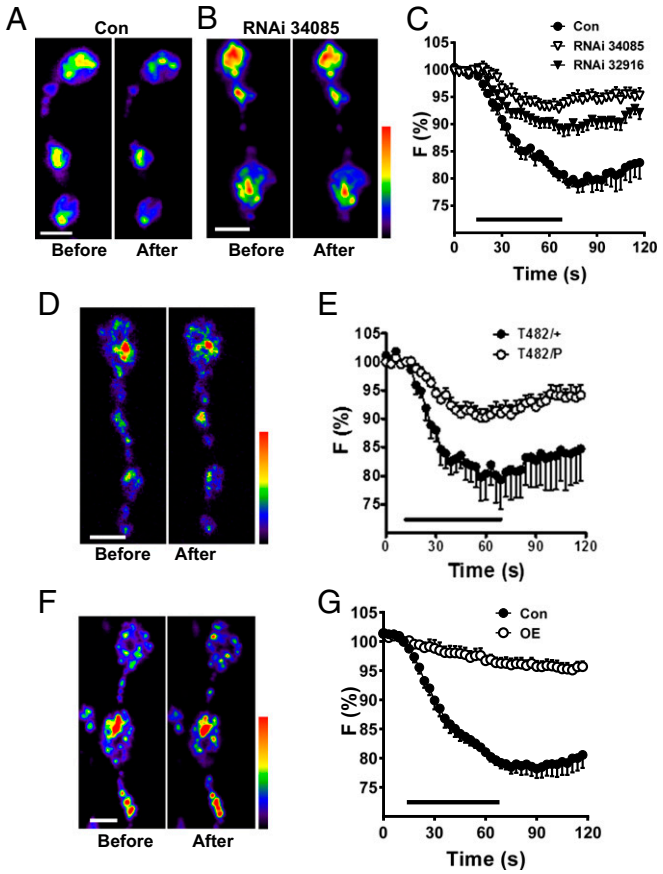

Fig. 3. Myopic regulates activity-induced synaptic neuropeptide release. Pseudocolor images of synaptic boutons expressing Dilp2-GFP in control animals (Con) (*A*) and Myopic RNAi (no. 34085) knockdown (*B*) before and after 70-Hz stimulation for 1 min. (*C*) Time-course DCV release in response to 70-Hz stimulation (indicated by bar) in Con and two lines of Myopic RNAi knockdown (RNAi, nos. 34085 and 32916) in synaptic boutons expressing Dilp2-GFP [Con (five animals); RNAi no. 34085 (12 animals), and RNAi no. 32916 (11 animals)]. F, fluorescence. (*D*) Pseudocolor images of heteroallelic (T482/P) Myopic mutant NMJs expressing Dilp2-GFP before and after 70-Hz stimulation. (*E*) Time-course DCV release in T482/+ (four animals) and Myopic mutant boutons (T482/P, nine animals) expressing Dilp2-GFP. (*F*) Pseudocolor images of boutons labeled with Dilp2-GFP overexpressing (OE) Myopic before and after stimulation. (*G*) Overexpression of Myopic (five animals) inhibits neuropeptide release in synaptic boutons (Con, six animals). (Scale bars, 2 μm.)

stores produced by perturbing Myopic expression reflect that optimal expression of Myopic facilitates activity-evoked synaptic neuropeptide release from DCVs.

Myopic Regulates Neuropeptide Release Evoked by Depolarization or cAMP. Release from DCVs is often associated with bursts of action potentials. Therefore, to determine if a change in action potential activity (e.g., frequency, pattern, waveform shape) underlies the Myopic effect, neuropeptide release was induced by tonic depolarization induced by application of elevated extracellular K^+. Even with this strong continuous depolarization, either knockdown or overexpression of Myopic reduced synaptic neuropeptide release (Fig. 4 *A–D*). Thus, release relies on optimal Myopic expression, and Myopic's effect cannot be attributed to a change in excitability.

This still left the possibility that Myopic affects a specific type of voltage-gated Ca^{2+} channel that is required for release from DCVs at the *Drosophila* NMJ (20) or intracellular Ca^{2+} release, buffering, or sensitivity. If Myopic controls the Ca^{2+} that stimulates release in response to activity or depolarization, then release induced independently of Ca^{2+} influx and cytosolic Ca^{2+} changes should be insensitive to perturbing Myopic expression. Therefore, cAMP in boutons was elevated by applying the adenylate cyclase activator forskolin in medium lacking Ca^{2+} and containing the Ca^{2+} chelator EGTA. Under these conditions, cytosolic Ca^{2+} is not elevated and cAMP-dependent protein kinase evokes synaptic neuropeptide release (21). Strikingly, cAMP-evoked synaptic neuropeptide release was inhibited dramatically by both knockdown and overexpression of Myopic (Fig. 4 *E–H*). This implies that Myopic does not act on Ca^{2+}, but rather affects the secretory machinery for stimulated DCV exocytosis that is shared by Ca^{2+} and cAMP.

Myopic Is Not Required for Synaptic Release by SSVs. Given the conserved secretory machinery for SSVs and DCVs, we then examined Myopic's participation in SSV-mediated release. Specifically, the styryl dye FM4-64 (4 μM) was loaded into SSVs by 70-Hz stimulation for 1 min, and release was evoked by an identical bout of electrical stimulation (Fig. 5*A*). In contrast to DCV-mediated neuropeptide release, SSV-mediated FM4-64 release evoked by activity was unaffected by either Myopic knockdown (Fig. 5 *B* and *D*) or overexpression (Fig. 5 *C* and *E*). Thus, Myopic is required selectively for exocytosis of synaptic DCVs.

This led us to examine localization of FLAG-tagged Myopic in synaptic boutons. Immunofluorescence was found in organelles that did not colocalize with DCVs (Fig. 5*F*). Localization was also inconsistent with SSVs (Fig. 5*A*). However, Myopic colocalized with the early endosome marker GFP-Rab5 (Fig. 5*G*). This is consistent with Myopic's role in ESCRT function. Therefore, we examined the effect of overexpressing a Bro1 double mutant that prevents Myopic interaction with the ESCRT III protein Shrub (CHMP4), which is implicated in neuron pruning (12). Interestingly, the mutant inhibited neuropeptide release as effectively as a matched wild-type Myopic construct [Fig. 5 *H–J*; half of that seen in Fig. 4*D*, control (Con)]. Thus, Myopic's differential effect on release from SSVs or DCVs cannot be attributed to selective association to either SSVs or DCVs or to a discriminating effect of ESCRT III.

Discussion

Neurotransmission depends on synaptic exocytosis of SSVs and DCVs. Extensive prior studies have failed to identify an exocytosis protein that is required selectively for only one of the two vesicle types underlying small-molecule transmitter/neuropeptide cotransmission. Thus, synaptic release has appeared to be mediated by conserved secretory machinery. Myopic has not been linked to DCVs specifically or exocytosis generally. Given this context, the dramatic effect of Myopic on DCV-mediated neuropeptide release was not expected. Myopic's impact on Ca^{2+}-independent cAMP-evoked neuropeptide release establishes that vesicle selectivity cannot be attributed to differential participation of Ca^{2+} channel subtypes or intracellular Ca^{2+} handling. Rather, Myopic regulates exocytosis of DCVs, but not SSVs. Unlike rab2 in *Caenorhabditis elegans* (22, 23), Myopic does not reduce DCV content to indirectly affect release. Thus, Myopic provides a molecular criterion for distinguishing classical and peptidergic transmission mechanisms at the NMJ.

It is intriguing that either decreasing or increasing Myopic expression produces comparable inhibition of synaptic neuropeptide release. The shared effect of up- and down-regulation is known for proteins that participate in complexes. Indeed, this is a defining characteristic of scaffold proteins (24, 25). Given that Myopic interacts with several functionally unrelated proteins (9, 10, 26), our results are consistent with a Myopic complex governing release by DCVs, but not SSVs. However, a Myopic

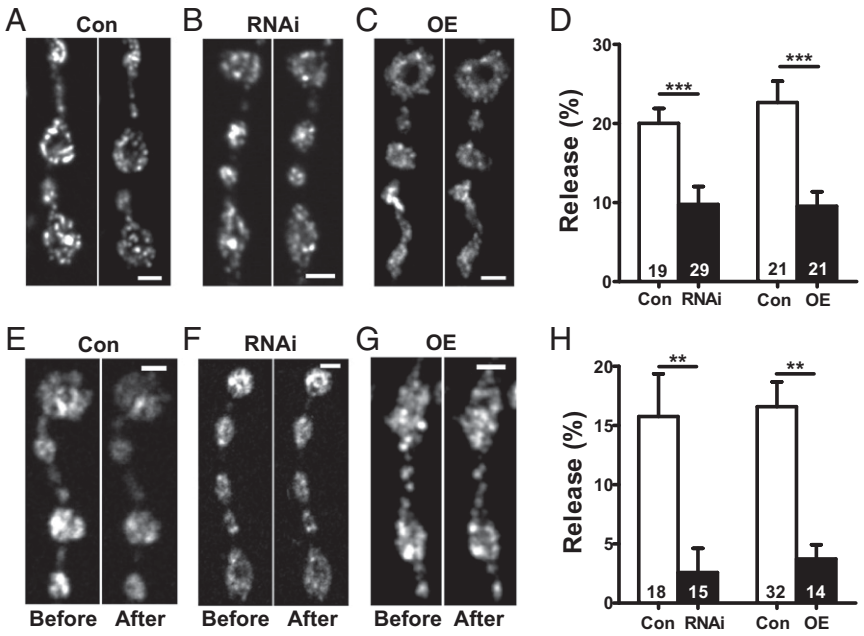

Fig. 4. Myopic regulates neuropeptide release evoked by depolarization and cAMP. (*A–C*) Representative images of Dilp2-GFP–expressing boutons in control (Con), RNAi knockdown (RNAi), and overexpressing Myopic (OE) animals before and after 2 min of KCl stimulation. (Scale bars, 2 μm.) (*D*) Quantification of depolarization-induced DCV release, measured as loss of Dilp2-GFP, in Myopic RNAi (no. 34085, four animals) and OE (five animals) NMJs using Bloomington no. 63120. Cons are from three animals each. Numbers on the bars represent the number of boutons analyzed. ***$P < 0.001$, unpaired *t* test. (*E–G*) Representative images of Dilp2-GFP–expressing boutons in Con, RNAi, and OE animals before and after 6 min of 50 μM forskolin exposure. (Scale bars, 2 μm.) (*H*) Quantification of forskolin-induced neuropeptide release, measured as loss of GFP, in Con, Myopic RNAi (five animals), and OE (six animals) NMJs. Control experiments for RNAi from were from seven animals, and experiments for OE were from 14 animals. Numbers on the bars represent the number of boutons analyzed. **$P < 0.01$, unpaired *t* test.

mutant shows that regulation of neuropeptide release is not mediated by Myopic association with the ESCRT III protein Shrub (CHMP4), which is required for Myopic's effect on neuron pruning (12). Thus, Myopic could act via another ESCRT complex or an ESCRT-independent mechanism. A provocative hypothesis is that the unknown Myopic complex influences kiss and run exocytosis, which exclusively mediates synaptic neuropeptide release at the *Drosophila* NMJ (27).

Because Myopic was studied with a neuropeptide reporter driven by the neuronal synaptobrevin promoter or the motoneuron driver OK6-GAL4, the release effect reported here is independent of native neuropeptide gene transcription. However, Myopic does, in fact, regulate the neuropeptide FMRFamide promoter as well as expression of the transcriptional cofactors Eya and pMad, which act with transcription factors to activate FMRFamide expression (14). Thus, Myopic acts at multiple levels (gene expression underlying cell specification and neuropeptide transcription and DCV exocytosis) to regulate peptidergic transmission. It will be of interest to determine whether these diverse Myopic effects are mediated by a single mechanism.

Materials and Methods

Neuropeptide Expression Construct and Transformation. The vector pUAS-C5 attB (28) was modified to remove upstream activating sequences (UASs) by digestion with SphI and PacI, and then blunted with T4 DNA polymerase and religated with T4 DNA ligase. The subsequent vector was digested with EcoRI and NotI, and EcoRI/NotI fragment containing Dilp2-GFP (15) was inserted. The vector was then digested with EcoRI and ligated with a 2-kb EcoRI fragment containing the upstream promoter region of nsyb (29). The complete vector was sent to Genetivision for insertion at the docking site VK1(2R)59D3. All restriction enzymes and DNA-modifying enzymes were purchased from New England Biolabs. One transformed stock was selected.

Fly Lines, Immunostaining, and Chemicals. As described above, Dilp2-GFP (15) was driven directly by the native neuronal synaptobrevin promoter to label DCVs in transgenic flies. This line was further modified by recombination with OK6-GAL4, which was used to drive UAS-Mop RNAi and overexpression constructs in motor neurons. For controls, UAS lines were crossed to the nsyb-Dilp2-GFP line without a GAL4 driver. For mop mutant studies, nsyb-Dilp2-GFP was crossed to w*; mop^{T482} P{neoFRT}80B/TM6B,Tb to generate a stock of w; nsyb-Dilp2-GFP/CyO; mop^{T482} P{neoFRT}80B/TM6B. This stock was then crossed to the mop allele y w; P{EPgy2}$mop^{EY06090}$, and non-Tb larvae with the mutant combination of mop^{T482}/P{EPgy2}$mop^{EY06090}$ were selected for analysis. ANF tagged with fluorescent timer protein monomeric mK-GO, which transitions from green to red fluorescence with age, was used to determine the age of DCVs (18). UAS-ANF-mK-GO was driven by 386Y-GAL4. UAS-Mop (no. 63120), UAS-Mop.Flag (no. 63119), w*; mop^{T482}/TM6B, Tb (no. 63118), y w; P{EPgy2}$mop^{EY06090}$ (no. 15817), and RNAi lines (nos. 32916 and 34085) were from the Bloomington Drosophila Stock Center. Darren W. Williams, King's College, London, provided the Bro1 domain double-mutant and matched wild-type UAS flies (12), which were crossed to nsyb-Dilp2-GFP, OK6-GAL4. Avital Rodal, Brandeis University, Waltham, MA, provided the vglut-GAL4; UAS-GFP-Rab5/TM6B,Tb flies, which were crossed to UAS-Mop.Flag.

For immunostaining, filleted larvae were fixed in 4% paraformaldehyde for 15 min and incubated with anti-FLAG M2 antibody (F1804; Sigma–Aldrich) at a 1:1,000 dilution, followed by Alexa 568 anti-mouse secondary antibody (A11004; Invitrogen) at a 1:500 dilution. Forskolin (F6886) was purchased from Sigma–Aldrich. FM4-64 was purchased from Invitrogen (T13320).

Imaging. As described previously (30, 31), imaging experiments were performed at type Ib synaptic boutons at muscle 6/7 of third-instar *Drosophila melanogaster* larvae, which do not endogenously express Dilp2. Animals were filleted in Ca^{2+}-free HL3 saline supplemented with 0.5 mM EGTA. For electrical stimulation experiments, they were transferred to HL3 saline that contained 70 mM NaCl, 5 mM KCl, 1.5 mM $CaCl_2$, 20 mM $MgCl_2$, 10 mM $NaHCO_3$, 5 mM trehalose, 115 mM sucrose, and 5 mM sodium Hepes (pH 7.2) supplemented with 10 mM L-glutamate to prevent muscle contractions. Nerve terminals were stimulated at 70 Hz via segmental nerves with a suction electrode. For KCl depolarization experiments 70 mM Na^+ was

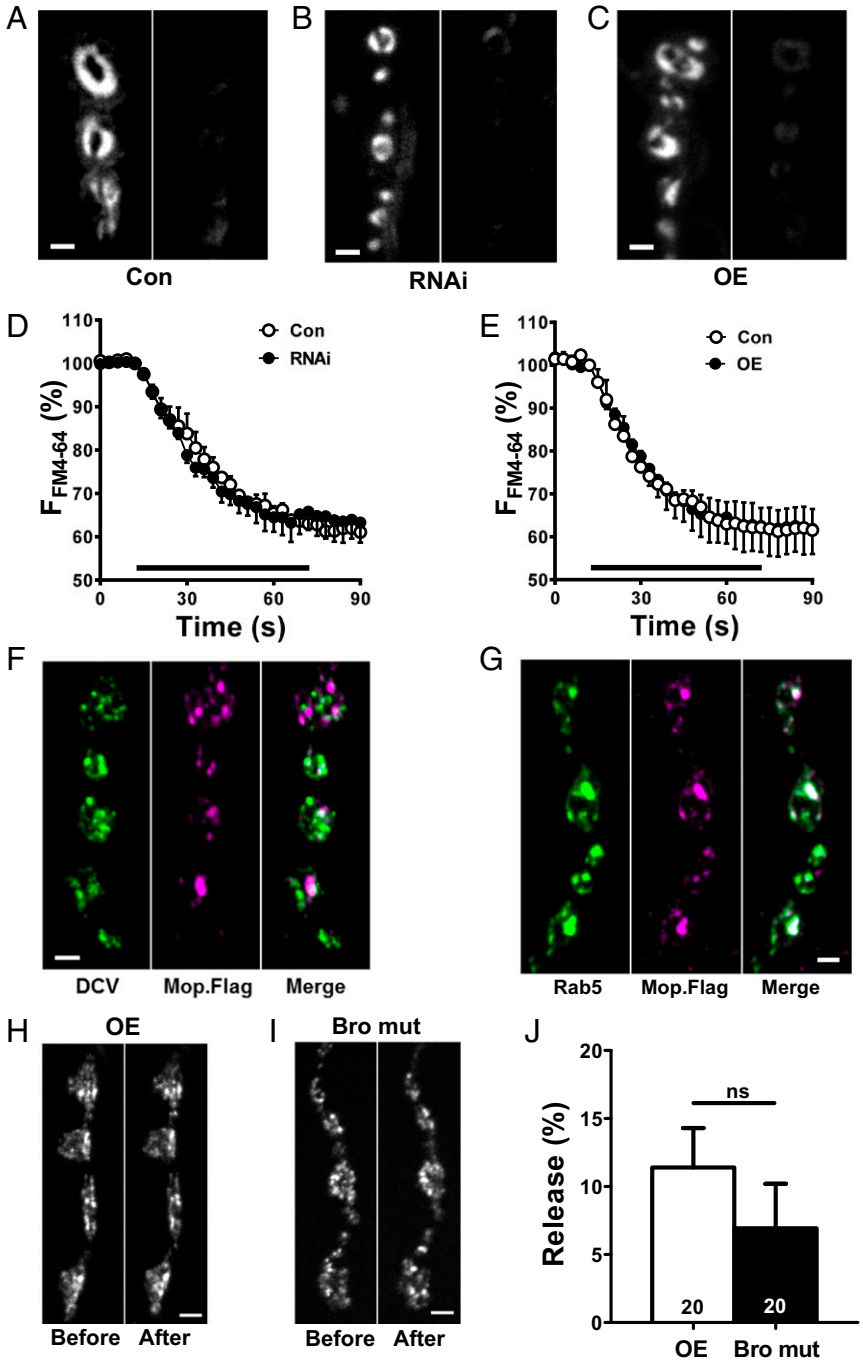

Fig. 5. Myopic is not required for synaptic release by SSVs. (*A–C*) Representative images of synaptic boutons loaded with FM4-64 in controls (Con), Myopic RNAi knockdown (RNAi; no. 34085) and overexpressing (OE) animals, before and after 70-Hz stimulation for 1 min. (Scale bars, 2 μm.) Time course of FM4-64 destaining in Con (three animals for each condition) and Myopic RNAi (six animals) (*D*) or OE (six animals) animals (*E*). F, fluorescence. (Bar, 70-Hz stimulation.) (*F*) Anti-FLAG staining of synaptic boutons expressing Dilp2-GFP (DCV) and FLAG-tagged Myopic (Mop.Flag). (*G*) GFP-tagged Rab5 is compared with Mop.Flag immunofluorescence. Results in *F* and *G* are representative of three animals. (Scale bars, 2 μm.) (*H* and *I*) Representative images showing Dilp2-GFP before and after 2 min of KCl stimulation in animals overexpressing matched wild-type (OE) and Bro domain mutant (Bro mut) (12). (Scale bars, 2 μm.) (*J*) Quantification from five OE and five Bro mut animals shows that release is equivalently inhibited (compare with Fig. 4*D*, Con). Numbers on the bars represent the number of boutons analyzed. ns, not significant by unpaired *t* test.

substituted with K^+. Data were acquired with a wide-field Olympus microscope equipped with a Yokogawa Spinning disk confocal module and a Hamamatsu EMCCD camera or with an Olympus Fluoview 1000 scanning confocal microscope. In mK-GO experiments, excitation was switched between 488-nm and 561-nm lasers, with simultaneous switching between green bandpass and red long-pass filters. Images were analyzed with ImageJ (NIH) software, while graphing was performed with Graphpad Prism software. DCV flux was determined by manually counting vesicles moving between neighboring boutons during time-lapse imaging acquired at 2 Hz.

Statistics. Statistical analysis was performed with Graphpad Prism software. Error bars represent SEM. The statistical comparison for two experimental groups was based on Student's *t* test. For more than two experimental

groups, one-way ANOVA with Dunnett's posttest was used for comparison with control.

ACKNOWLEDGMENTS. We thank Drs. Richard Daniels and Barry Ganetzky (University of Wisconsin) for providing the pUAS-C5 attB plasmid, Dr. Darren W. Williams (King's College) for the Bro1 domain mutant and matched control UAS lines, Dr. Avital Rodal (Brandeis University) for the vglut>GFP-Rab5 flies, and Samantha Cavolo for technical assistance. Stocks obtained from the Bloomington Drosophila Stock Center (NIH Grant P40OD018537) were used in this study. This research was supported by NIH Grant R01 NS032385 (to E.S.L.).

1. Nusbaum MP, Blitz DM, Marder E (2017) Functional consequences of neuropeptide and small-molecule co-transmission. *Nat Rev Neurosci* 18:389–403.
2. Rettig J, Neher E (2002) Emerging roles of presynaptic proteins in Ca++-triggered exocytosis. *Science* 298:781–785.
3. Jahn R, Lang T, Südhof TC (2003) Membrane fusion. *Cell* 112:519–533.
4. Sørensen JB (2004) Formation, stabilisation and fusion of the readily releasable pool of secretory vesicles. *Pflugers Arch* 448:347–362.
5. James DJ, Martin TF (2013) CAPS and Munc13: CATCHRs that SNARE vesicles. *Front Endocrinol (Lausanne)* 4:187.
6. Doyotte A, Mironov A, McKenzie E, Woodman P (2008) The Bro1-related protein HD-PTP/PTPN23 is required for endosomal cargo sorting and multivesicular body morphogenesis. *Proc Natl Acad Sci USA* 105:6308–6313.
7. Miura GI, Roignant JY, Wassef M, Treisman JE (2008) Myopic acts in the endocytic pathway to enhance signaling by the Drosophila EGF receptor. *Development* 135: 1913–1922.
8. Gingras MC, et al. (2009) HD-PTP is a catalytically inactive tyrosine phosphatase due to a conserved divergence in its phosphatase domain. *PLoS One* 4:e5105.
9. Gingras MC, Kazan JM, Pause A (2017) Role of ESCRT component HD-PTP/PTPN23 in cancer. *Biochem Soc Trans* 45:845–854.
10. Gilbert MM, Tipping M, Veraksa A, Moberg KH (2011) A screen for conditional growth suppressor genes identifies the Drosophila homolog of HD-PTP as a regulator of the oncoprotein Yorkie. *Dev Cell* 20:700–712.
11. Husedzinovic A, et al. (2015) The catalytically inactive tyrosine phosphatase HD-PTP/PTPN23 is a novel regulator of SMN complex localization. *Mol Biol Cell* 26:161–171.
12. Loncle N, Agromayor M, Martin-Serrano J, Williams DW (2015) An ESCRT module is required for neuron pruning. *Sci Rep* 5:8461.
13. Pradhan-Sundd T, Verheyen EM (2015) The Myopic-Ubpy-Hrs nexus enables endosomal recycling of Frizzled. *Mol Biol Cell* 26:3329–3342.
14. Bivik C, et al. (2015) Novel genes involved in controlling specification of *Drosophila* FMRFamide neuropeptide cells. *Genetics* 200:1229–1244.
15. Wong MY, et al. (2012) Neuropeptide delivery to synapses by long-range vesicle circulation and sporadic capture. *Cell* 148:1029–1038.
16. Shakiryanova D, Tully A, Levitan ES (2006) Activity-dependent synaptic capture of transiting peptidergic vesicles. *Nat Neurosci* 9:896–900.
17. Tsuboi T, Kitaguchi T, Karasawa S, Fukuda M, Miyawaki A (2010) Age-dependent preferential dense-core vesicle exocytosis in neuroendocrine cells revealed by newly developed monomeric fluorescent timer protein. *Mol Biol Cell* 21:87–94.
18. Bulgari D, Zhou C, Hewes RS, Deitcher DL, Levitan ES (2014) Vesicle capture, not delivery, scales up neuropeptide storage in neuroendocrine terminals. *Proc Natl Acad Sci USA* 111:3597–3601.
19. Tao J, Bulgari D, Deitcher DL, Levitan ES (2017) Limited distal organelles and synaptic function in extensive monoaminergic innervation. *J Cell Sci* 130:2520–2529.
20. James RE, et al. (2014) Crimpy enables discrimination of presynaptic and postsynaptic pools of a BMP at the Drosophila neuromuscular junction. *Dev Cell* 31:586–598.
21. Shakiryanova D, Zettel GM, Gu T, Hewes RS, Levitan ES (2011) Synaptic neuropeptide release induced by octopamine without Ca^{2+} entry into the nerve terminal. *Proc Natl Acad Sci USA* 108:4477–4481.
22. Edwards SL, et al. (2009) Impaired dense core vesicle maturation in Caenorhabditis elegans mutants lacking Rab2. *J Cell Biol* 186:881–895.
23. Sumakovic M, et al. (2009) UNC-108/RAB-2 and its effector RIC-19 are involved in dense core vesicle maturation in Caenorhabditis elegans. *J Cell Biol* 186:897–914.
24. Burack WR, Shaw AS (2000) Signal transduction: Hanging on a scaffold. *Curr Opin Cell Biol* 12:211–216.
25. Good MC, Zalatan JG, Lim WA (2011) Scaffold proteins: Hubs for controlling the flow of cellular information. *Science* 332:680–686.
26. Gahloth D, et al. (2017) The open architecture of HD-PTP phosphatase provides new insights into the mechanism of regulation of ESCRT function. *Sci Rep* 7:9151.
27. Wong MY, Cavolo SL, Levitan ES (2015) Synaptic neuropeptide release by dynamin-dependent partial release from circulating vesicles. *Mol Biol Cell* 26:2466–2474.
28. Daniels RW, Rossano AJ, Macleod GT, Ganetzky B (2014) Expression of multiple transgenes from a single construct using viral 2A peptides in Drosophila. *PLoS One* 9: e100637.
29. Rao SS, et al. (2001) Two distinct effects on neurotransmission in a temperature-sensitive SNAP-25 mutant. *EMBO J* 20:6761–6771.
30. Shakiryanova D, Tully A, Hewes RS, Deitcher DL, Levitan ES (2005) Activity-dependent liberation of synaptic neuropeptide vesicles. *Nat Neurosci* 8:173–178.
31. Levitan ES, Lanni F, Shakiryanova D (2007) In vivo imaging of vesicle motion and release at the Drosophila neuromuscular junction. *Nat Protoc* 2:1117–1125.